

Pseudogap in the chain states of YBCO

V. B. Zabolotnyy,¹ A. A. Kordyuk,¹ D. Evtushinsky,¹ V. N. Strocov,² L. Patthey,² T. Schmitt,²
D. Haug,³ C. T. Lin,³ V. Hinkov,^{4,3} B. Keimer,³ B. Büchner,¹ and S. V. Borisenko¹

¹*Institute for Solid State Research, IFW-Dresden, P.O. Box 270116, D-01171 Dresden, Germany*

²*Paul Scherrer Institut, Swiss Light Source, CH-5232 Villigen PSI, Switzerland*

³*Max-Planck-Institut für Festkörperforschung, HeisenbergstraSe 1, 70569 Stuttgart, Germany*

⁴*Quantum Matter Institute, University of British Columbia, Vancouver, B.C. V6T 1Z1, Canada*

As established by scanning tunneling microscopy (STM) cleaved surfaces of the high temperature superconductor $\text{YBa}_2\text{Cu}_2\text{O}_{7-\delta}$ develop charge density wave (CDW) modulations in the one-dimensional (1D) CuO chains. At the same time, no signatures of the CDW have been reported in the spectral function of the chain band previously studied by photoemission. We use soft X-ray angle resolved photoemission (SX-ARPES) to detect a chain-derived surface band that had not been detected in previous work. The $2k_F$ for the new surface band is found to be 0.55 \AA^{-1} , which matches the wave vector of the CDW observed in direct space by STM. This reveals the relevance of the Fermi surface nesting for the formation of CDWs in the CuO chains in $\text{YBa}_2\text{Cu}_2\text{O}_{7-\delta}$. In agreement with the short range nature of the CDW order the newly detected surface band exhibits a pseudogap, whose energy scale also corresponds to that observed by STM.

PACS numbers: 71.45.Lr, 74.72.Kf, 79.60.-i, 79.60.Jv

The CuO chain structure in $\text{YBa}_2\text{Cu}_2\text{O}_{7-\delta}$ (Y-123) provides a physical realization of a quasi-one-dimensional electronic system with non-vanishing coupling to the CuO_2 bilayers.^{1,2} One of the reasons why 1D electronic systems remain in the focus of solid state research is that even weak interactions transform the quasi-particles of Fermi liquid theory into collective excitations of density wave type.³⁻⁵ In particular, the peculiar topological structure of the chain Fermi surface (FS) makes this electronic system prone to formation of charge density wave via the Peierls instability.⁶ Indeed, charge density modulations along the Cu-O chains have been extensively studied probing cleaved surfaces of Y-123 in direct space with scanning tunneling microscopy.⁷⁻¹⁵ It has been shown that Y-123 crystals cleave between the CuO chains and the BaO layer, so that the chains turn out to be the nearest to the surface building block.^{7,9,10,15} Both the earliest⁹ and the most recent studies¹⁴ present a consistent picture of a CDW, appearing as corrugations of the electronic density with a short correlation range of about 40 \AA and a period between 9 and 14 \AA , depending on the sample stoichiometry.

In the case of 2D systems, the effect of CDW on the electronic states in the reciprocal space has been examined in great detail with modern angle resolved spectroscopy, which provides both momentum and energy resolution when measuring the one particle spectral function. Occurrences of the pseudogap for an incommensurate (or short range ordered) state, which finally develops into a true CDW band gap below T_{CDW} , are well documented.¹⁶⁻¹⁹ In the case of 1D systems other than Y-123, modifications to the spectral function with the onset of the CDW state have been detected as well.²⁰⁻²² the emergence of a pseudogap-like state is also expected in theory and can be understood as a result of a fluctuating Peierls order parameter.²³⁻²⁷

At the same time, despite the abundant evidence for charge modulations in direct space provided by STM, Y-123 chains seem to exhibit neither a pseudogap nor the Tomonaga-Luttinger behavior observed in the related

$\text{PrBa}_2\text{Cu}_4\text{O}_8$.^{28,29} Momentum resolved spectra measured from as-cleaved Y-123 surfaces,³⁰⁻³² as well as those measured on the *in situ* doped ones³³ manifest neither folding nor notable suppression of the spectral weight at the Fermi level. That is, the spectral features that could be regarded as signatures of the CDW state are absent in spectra of Y-123. Therefore, it remains unclear why the two complementary methods (STM and ARPES) deliver such conflicting results.

To address this problem we have investigated high quality Y-123 crystals using modern SX-ARPES. the photoemission data for this study were collected at the recently built high-resolution soft X-ray beamline ADDRESS at the Swiss Light Source.³⁴ This beamline delivers photon flux up to 10^{13} ph/s in an energy window of 0.01% of photon energy. Such a high flux allows one to break through the problem of dramatic reduction of the valence band cross section at high photon energies. the samples were mounted on a low-temperature goniometric manipulator (CARVING) with three angular degrees of freedom and cleaved *in situ* in ultrahigh vacuum with base pressure better than $5 \cdot 10^{-11}$ mBar at $T=10$ K, the same temperature at which all the spectra were acquired. The energy resolution depends on the kinetic energy and will be stated in the figure captions, details of the SX-ARPES station will be published elsewhere.³⁵ The experiments were performed using high-quality single crystals of $\text{Ba}_2\text{Cu}_3\text{O}_{6.6}$ ($T_c \approx 61$ K) from the same batch as in the recent INS study.³⁶ The crystals were synthesized by the solution-growth technique, annealed to the desired oxygen doping, and detwinned by applying uniaxial mechanical stress at elevated temperature.³⁶

As a result of the ‘surface polar catastrophe’³³ the electronic structure of the Y-123 surface layer is known to be different from that of the bulk.³⁷ Generally, there are two major approaches that have been used in photoemission practice to highlight bulk states against the surface ones. Surface aging is the first option, which basically relies on the destruction of surface states.^{38,39} The other approach employs the variation of photon excitation energy and po-

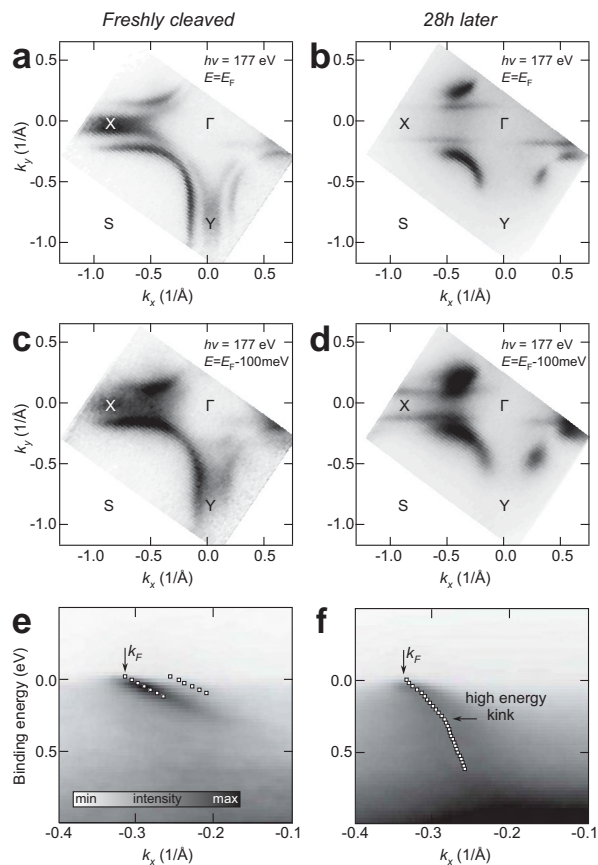


FIG. 1: Sample aging. (a), (b) FS maps measured directly after cleavage and 28 hours later. (c), (d) Corresponding fresh and aged intensity distributions for constant energy cuts at $E = E_F - 100$ meV. (e), (f) Energy-momentum intensity distributions along the Γ -S direction. The white squares are the result of MDC fits. Dark corresponds to high photoemission intensity. Spectra measured at $T = 10$ K with 38 meV energy resolution using linearly s -polarised light (i.e. no out of plane component of the polarization vector).

larization, which affect the inelastic escape depth of exited electrons^{40–42} and the ratio of photoemission matrix elements for bulk and surface states.^{32,43} Also the rapid variation in the elastic scattering rate with the kinetic energy of the excited photoelectrons may play a decisive role.^{44,45}

We start out the discussion of experimental data with an illustration of the first option. Fig. 1 contains a comparison of the Fermi surfaces measured from the freshly cleaved sample to the same measurement done 28 hours after the cleavage. The freshly cleaved surface results in a typical picture of bilayer split FS contours corresponding to the CuO_2 plane states (rounded double squares centered at S point) and the quasi-one-dimensional chain band (faint features running parallel to the k_x axis). After surface degradation there are some notable changes.

First, the overdoped CuO_2 plane bands are replaced with the ‘Fermi arc’ features similar to those observed in refs. 46, 47. The appearance of the ‘Fermi arcs’ is also accompanied by a k_F shift (Fig. 1(e–f)). For the bonding band, it can

be estimated from the MDC fits, and amounts to about $\delta k_F \approx 0.04 \text{ \AA}$ along the Γ -S direction. Assuming the same shrinking over the whole Fermi surface and an average FS radius $k_F \approx 0.55 \text{ \AA}$, one may estimate the decrease in hole doping as $\delta p \approx 4\pi k_F \delta k_F / S_{\text{BZ}} \approx 0.1$, which brings us from the typically overdoped regime with $p \approx 0.3$ (refs. 30,31,38,48) under the superconducting dome with $p \approx 0.2$. Note also the so called ‘waterfalls’ and a high energy kink at about 250 meV, which have recently generated an avalanche of publications.^{49–52} These issues are beyond the scope of the current study, and we do not further elaborate on them here.

Second, the relative intensity of the 1D chain band as compared to the 2D bands is substantially increased, while the distance between the chain Fermi crossings, $2k_F$, remains practically the same. This suggests that the observed chain band is most likely a ‘bulk’ feature, in a sense that it originates from the chain structure protected by at least one CuO_2 bilayer, and not from the cleaved chains. Since the upper neighboring CuO_2 bilayers turn out to be overdoped, the electronic structure of these chains still differs from LDA band structure calculation,² so in the following we will refer to these chains as subsurface ones, in order to contrast this structure with the chains through which the cleavage takes place and the true bulk chains.

This observation is consistent with the interpretation given in ref. 32, which was based on the pattern of circular dichroism. This work has shown that the chain signal observed in ARPES experiment mainly originates from the nearest to the surface *undisturbed* chains protected by the overdoped CuO_2 bilayer, so that the surface aging is expected to enhance the photoemission from these chain

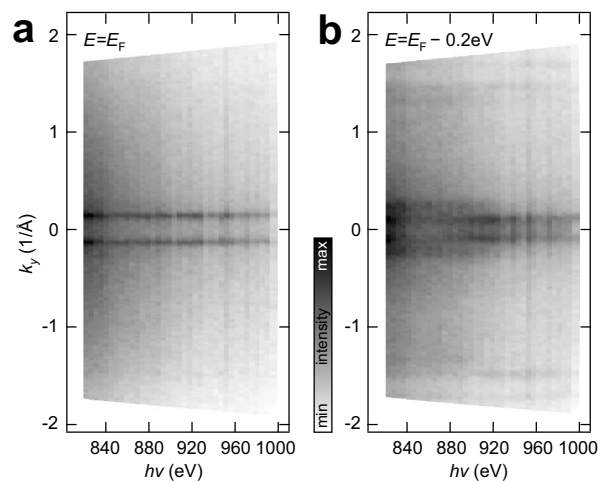


FIG. 2: Excitation energy dependence for the cut passing through the Γ point parallel to the k_y axis. The left panel shows the intensity integrated around the Fermi level, $E = E_F$. The right image contains intensity at 200 meV below the Fermi level, demonstrating another set of chain features for $h\nu \lesssim 920$ eV. Spectra were measured using p -polarized light with overall energy resolution of 125 meV.

states as compared to other surface features. Though there are intensity variations along the chain band, it is noteworthy that the band exhibits neither pseudogap nor folding phenomena. As can be seen in Fig. 1(a–d), there are no indications for a CDW state for the freshly cleaved and aged surfaces.

Now we turn to the discussion of the second option. Searching for the signatures of a CDW in Y-123 spectra we have measured the excitation energy dependence for the Y– Γ –Y cut, the one where only a parabolic chain band is expected to cross the FL.² Fig. 2 contains the intensity distribution for that direction plotted at the FL (a) and 200 meV below the FL (b). While the data in panel (a) exhibit only two parallel features, corresponding to the $\pm k_F$ crossings of the two branches of the parabolic chain band, the intensity distribution in Fig. 2(b) reveals another set of features running parallel with a slightly larger separation. The new features are well visible at low excitation energies $h\nu \lesssim 920$ eV, therefore based on the universal dependence of the escape depth one may assume the new feature to be a surface related one. However, the decrease of the photoemission intensity from the surface chain band as compared to the subsurface ones occurs rather abruptly, whereas the universal escape depth curve predicts smooth $\propto E_{\text{kin}}^{1/2}$ dependence, where E_{kin} is the kinetic energy of the excited photoelectrons. Therefore this observation cannot be solely attributed to the electron escape depth, so also the $h\nu$ dependence of the photoemission matrix elements needs to be taken into account. In contrasting surface photoemission with bulk emission, particular attention has to be paid to the surface induced light fields, which are likely to be responsible for the different $h\nu$ dependence of the matrix elements for surface and bulk localized states.^{53–55} For instance, the absence of the new surface chain states in the spectra shown in Fig. 1 would be consistent with the fact that these spectra were measured with *s*-polarized light. For this polarization there is no component of the exciting field $\mathbf{A}(\mathbf{r})$ perpendicular to the sample surface, and hence the surface related term in the photoemission matrix element $\langle f | \mathbf{A} \nabla + \frac{1}{2} \text{div} \mathbf{A} | i \rangle$ is negligible, rendering the surface emission effects irrelevant as compared to the case of *p*-polarized light.

To establish the dimensionality and topology of this previously overlooked surface state, in Fig. 3(a,b) we plot a FS measured with 620 eV photons and corresponding iso-energy intensity distribution taken 100 meV below the FL. According to the $h\nu$ dependence, the new feature is expected to have significant contribution to the experimental spectra at this energy. As can be seen, the new band practically does not contribute spectral weight at the FL (pseudogapped), though at 100 meV binding energy the band gives rise to two 1D traces similar to those spawned by the chain band. This suggests that the subsurface chains and the pseudogapped surface feature stem from homologous bands with, probably, different spatial localization. Indeed, a detailed analysis of the LDA band structure² shows that there are no other 1D bands except for the chains that the pseudogapped feature could be attributed to. Further, k_z dispersion cannot be

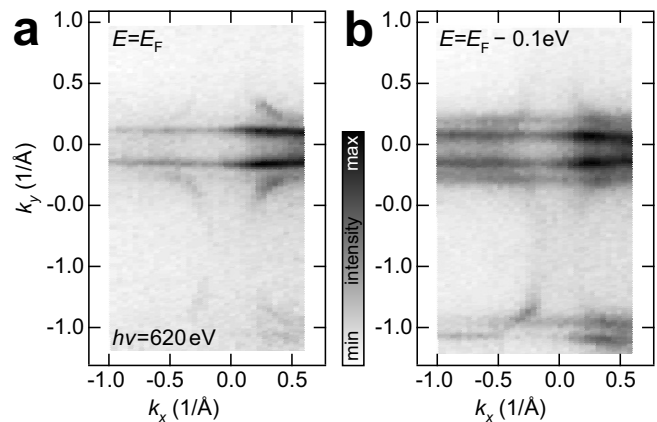


FIG. 3: (a), (b) Momentum intensity distribution at the Fermi level and at 0.1 eV below the FL. The right image reveals another 1D band, which contributes practically no spectral weight at the Fermi level. Spectra measured with *p*-polarized light and energy resolution of 90 meV.

responsible for the appearance of the second pseudogapped chain band in the spectrum, since along the Y– Γ –Y direction the calculated $k_{F\parallel}$ variation with k_z ($\pm 4\%$ $k_{F\parallel}$) is notably smaller than the observed splitting.

In Fig. 4(a, b) we plot the energy–momentum intensity distribution for the Y– Γ –Y direction. Panel (b) contains the same data set, but each MDC making up the image has been normalized to a fixed value, in order to show the band dispersion in the region that is ‘overexposed’ in panel (a).

The inner band with $2k_F \sim 0.28 \text{ \AA}^{-1}$ is the chain band that we attribute here to the subsurface chain states, and the outer one, with $2k_F \sim 0.55 \text{ \AA}^{-1}$ is the newly observed band, which we believe to be a surface localized chain band. The suppression of the spectral weight down to about 250 meV for the surface chains as compared to the bulk ones is clearly visible. In the panel (c) we additionally compare two EDC’s taken at the effective k_F of the bulk and surface bands, which once again demonstrate the pseudogap-like suppression of the spectral weight for the surface band. While for the subsurface chains the spectral intensity grows approximately as the Fermi function convoluted with experimental resolution, for the surface band a gradual growth of intensity is observed. The estimated energy scale is about 200–300 meV.

In the case of true CDW gap, using model calculations, it has been demonstrated that new states arise on the order of $E_F \pm \Delta$. For these energies, the CDW component of the local DOS was shown to have a characteristic amplitude and phase.⁵⁶ Extending this results on the pseudogap, we note that the pseudogap nicely agrees with the STM results of ref. 7 and ref. 12. Namely, the charge corrugations are visible for bias voltages up to 310 meV and practically vanish for bias voltages higher than 480 meV. In this regard we can also conclude that another small gap (~ 20 meV) observed in STM spectra and attributed either to CDW gap or to proximity induced superconducting gap,⁸ is likely to be a superconductivity related one.

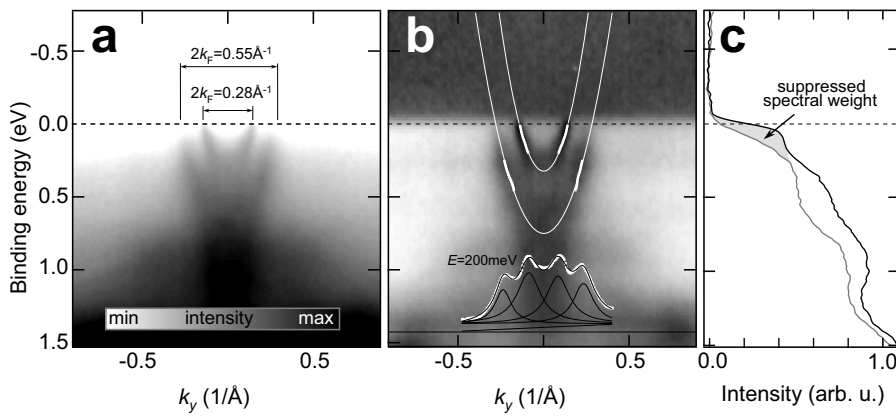


FIG. 4: (a) Energy-momentum cut along the Y- Γ -Y direction demonstrating two types of chain bands. (b) The same as previous, but each MDC in the image has been normalized to one. The small square symbols denote the peak positions obtained in a four-Lorentzian MDC fit. The insert shows typical fit for the MDC at $E_B=200$ meV. The obtained experimental dispersions are fit to parabolic bands (solid white lines). (c) k_F EDC's for the inner chain band (black line) and outer chain band (grey line). Polarization and resolution are the same as in Fig. 3.

It is also informative to see how the observed band dispersion compares to the CDW modulations measured in STM experiment. Simple theory predicts that the CDW wave vector should be twice the Fermi vector, $q_{\text{CDW}} = 2\pi/\lambda_{\text{CDW}} = 2k_F$. To estimate from the photoemission spectrum where the pseudogapped chain band would cross the FL, if there were no CDW instability, we use the result of an MDC fit performed for energies below the gapped region (white symbols in Fig. 4(b)) and extrapolate the experimental points up to the Fermi level assuming a parabolic dispersion. The value thus obtained is $2k_F = 0.55 \text{ \AA}^{-1}$, which yields $\lambda_{\text{CDW}} = 11.4 \text{ \AA}$. This value nicely compares to the $\lambda = 11.2 \text{ \AA}$, observed in Zn substituted Y-123.¹² It is also within the range of CDW periods from 9 to 14 \AA reported for a series of $\text{YBa}_2\text{Cu}_2\text{O}_{7-\delta}$ samples with varying stoichiometry,¹¹ approximately corresponding to the sample with $\delta = 0.35$ used in that study.

At the same time for the subsurface chains with $2k_F = 0.28 \text{ \AA}^{-1}$, so the expected CDW period would be about 22 \AA , which obviously does not match the STM data. Together with the absence of the (pseudo)gap this once again suggests that CDW modulations, which have been studied in so many details by STM, are due to the $2k_F = 0.55 \text{ \AA}^{-1}$ instability occurring in the previously overlooked surface chain band. Disorder in the chain structure results in a short range character of the CDW and the development of the pseudogap in the chain band.

It is remarkable that the chains at the surface develop the CDW state, while the neighboring chains sandwiched between the overdoped and bulk CuO_2 layers display no notable signatures of the CDW. One reason for this could be a trivial difference in phonon modes available at the surface and in the bulk. However commensuration effects

appear to be of no less importance. As compared to the incommensurate state, there is an additional energy lowering associated with the commensurability of the CDW state, which is not taken into account in the simplest variant of the CDW theory.^{6,57} The energy gain is given by $E_{\text{comm}} = -\frac{n(\epsilon_F)\Delta^2}{\lambda_{\text{el-ph}}} \left(\frac{\Delta}{D}\right)^{M-2}$. Here D is the band width, Δ is the CDW gap, $\lambda_{\text{el-ph}}$ is the electron-phonon coupling constant, $n(\epsilon_F)$ - density of states at the Fermi level, and $M = \lambda_{\text{CDW}}/a$ is the commensurability factor. As can be seen the correction is most significant at low M values. Considering this correction, for the surface chains we have $M \approx 11.4/3.89 \approx 2.94$, which is indistinguishable from a commensurate modulation with $M = 3$. For the subsurface chains $M = 5.77$ is quite large and differs significantly from the nearest commensurate value $M = 6$. Consequently the E_{comm} correction is negligible in this case, which obviously should affect the energy balance, making the CDW phase less favorable for the subsurface chains.

In conclusion, we have identified the origin of the CDW observed at the surface of Y-123 by STM by detecting a previously overlooked 1D surface band in Y-123, which brings into agreement two complementary methods: ARPES and STM. As a result of a Peierls instability, the surface CuO chain band develops a short range CDW state, which results in the appearance of a pseudogap in the one particle excitation spectrum detected in our ARPES experiment. Both energy and momentum scales measured in STM and ARPES are found to be in agreement with each other.

We thank F. Dubi and C. Hess for technical support during the measurements. The project was supported in part by DFG grant ZA 654/1-1.

¹ O. K. Andersen, A. I. Liechtenstein, O. Jepsen, and F. Paulsen, *Journal of Physics and Chemistry of Solids* **56**, 1573 (1995) Proceedings of the Conference on Spectroscopies in Novel Superconductors.

² W. E. Pickett, R. E. Cohen, and H. Krakauer, *Phys. Rev. B* **42**, 8764 (1990).

³ S. Tomonaga, *Prog. Theor. Phys.* **5**, 544 (1950).

⁴ J. M. Luttinger, *Phys. Rev.* **4**, 1154 (1963).

⁵ V. Meden and K. Schönhammer, *Phys. Rev. B* **46**, 15753 (1992).

⁶ G. Grüner, *Density Waves in Solids* Addison-Wesley, Reading, MA, 1994.

⁷ H. L. Edwards, A. L. Barr, J. T. Markert, and A. L. de Lozanne,

- Phys. Rev. Lett.* **73**, 1154 (1994).
- ⁸ H. L. Edwards, D. J. Derro, A. L. Barr, J. T. Markert, and A. L. de Lozanne, *Phys. Rev. Lett.* **75**, 1387 (1995).
 - ⁹ H. L. Edwards, J. T. Markert, and A. L. de Lozanne, *Phys. Rev. Lett.* **69**, 2967 (1992).
 - ¹⁰ M. Maki, T. Nishizaki, K. Shibata, and N. Kobayashi, *J. Phys. Soc. Jpn.* **70**, 1877 (2001).
 - ¹¹ M. Maki, T. Nishizaki, K. Shibata, and N. Kobayashi, *Phys. Rev. B* **65**, 140511 (2002).
 - ¹² M. Maki, T. Nishizaki, K. Shibata, and N. Kobayashi, *Phys. Rev. B* **72**, 024536 (2005).
 - ¹³ M. Maki, T. Nishizaki, K. Shibata, and N. Kobayashi, *Physica C: Superconductivity* **378-381**, 84 (2002).
 - ¹⁴ D. J. Derro, E. W. Hudson, K. M. Lang, S. H. Pan, J. C. Davis, J. T. Markert, and A. L. de Lozanne, *Phys. Rev. Lett.* **88**, 097002 (2002).
 - ¹⁵ G. Urbanik, T. Hänke, C. Hess, B. Büchner, A. Ciszewski, V. Hinkov, C. T. Lin, and B. Keimer, *The European Physical Journal B - Condensed Matter and Complex Systems* **69**, 483 (2009).
 - ¹⁶ M. Bovet, D. Popović, F. Clerc, C. Koitzsch, U. Probst, E. Bucher, H. Berger, D. Naumović, and P. Aebi, *Phys. Rev. B* **69**, 125117 (2004).
 - ¹⁷ T. Yokoya, T. Kiss, A. Chainani, S. Shin, and K. Yamaya, *Phys. Rev. B* **71**, 140504 (2005).
 - ¹⁸ S. V. Borisenko, A. A. Kordyuk, A. N. Yaresko, V. B. Zabolotnyy, D. S. Inosov, R. Schuster, B. Büchner, R. Weber, R. Follath, L. Patthey, and H. Berger, *Phys. Rev. Lett.* **100**, 196402 (2008).
 - ¹⁹ S. V. Borisenko, A. A. Kordyuk, V. B. Zabolotnyy, D. S. Inosov, D. Evtushinsky, B. Büchner, A. N. Yaresko, A. Varykhalov, R. Follath, W. Eberhardt, L. Patthey, and H. Berger, *Phys. Rev. Lett.* **102**, 166402 (2009).
 - ²⁰ J. Schäfer, M. Sing, R. Claessen, E. Rotenberg, X. J. Zhou, R. E. Thorne, and S. D. Kevan, *Phys. Rev. Lett.* **91**, 066401 (2003).
 - ²¹ A. Koitzsch, D. S. Inosov, H. Shiozawa, V. B. Zabolotnyy, S. V. Borisenko, A. Varykhalov, C. Hess, M. Knupfer, U. Ammerahl, A. Revcolevschi, and B. Büchner, *Phys. Rev. B* **81**, 113110 (2010).
 - ²² K. N. Altmann, J. N. Crain, A. Kirakosian, J.-L. Lin, D. Y. Petrovykh, F. J. Himpsel, and R. Losio, *Phys. Rev. B* **64**, 035406 (2001).
 - ²³ L. Bartosch and P. Kopietz, *Phys. Rev. Lett.* **82**, 988 (1999).
 - ²⁴ L. Bartosch and P. Kopietz, *Phys. Rev. B* **60**, 15488 (1999).
 - ²⁵ L. Bartosch and P. Kopietz, *Phys. Rev. B* **62**, R16223 (2000).
 - ²⁶ A. J. Millis and H. Monien, *Phys. Rev. B* **61**, 12496 (2000).
 - ²⁷ L. Bartosch, *Annalen der Physik* **10**, 799 (2001).
 - ²⁸ T. Mizokawa, C. Kim, Z.-X. Shen, A. Ino, A. Fujimori, M. Goto, H. Eisaki, S. Uchida, M. Tagami, K. Yoshida, A. I. Rykov, Y. Siohara, K. Tomimoto, and S. Tajima, *Phys. Rev. B* **60**, 12335 (1999).
 - ²⁹ T. Mizokawa, K. Nakada, C. Kim, Z.-X. Shen, T. Yoshida, A. Fujimori, S. Horii, Y. Yamada, H. Ikuta, and U. Mizutani, *Phys. Rev. B* **65**, 193101 (2002).
 - ³⁰ K. Nakayama, T. Sato, K. Terashima, H. Matsui, T. Takahashi, M. Kubota, K. Ono, T. Nishizaki, Y. Takahashi, and N. Kobayashi, *Phys. Rev. B* **75**, 014513 (2007).
 - ³¹ V. B. Zabolotnyy, S. V. Borisenko, A. A. Kordyuk, J. Geck, D. S. Inosov, A. Koitzsch, J. Fink, M. Knupfer, B. Büchner, S.-L. Drechsler, H. Berger, A. Erb, M. Lambacher, L. Patthey, V. Hinkov, and B. Keimer, *Phys. Rev. B* **76**, 064519 (2007).
 - ³² V. B. Zabolotnyy, S. V. Borisenko, A. A. Kordyuk, D. S. Inosov, A. Koitzsch, J. Geck, J. Fink, M. Knupfer, B. Büchner, S.-L. Drechsler, V. Hinkov, B. Keimer, and L. Patthey, *Phys. Rev. B* **76**, 024502 (2007).
 - ³³ M. A. Hossain, J. D. F. Mottershead, D. Fournier, A. Bostwick, J. L. McChesney, J. L. McChesney, E. Rotenberg, R. Liang, W. N. Hardy, G. A. Sawatzky, I. S. Elfimov, D. A. Bonn, and A. Damascelli, *Nature Phys.* **4**, 527 (2008).
 - ³⁴ V. N. Strocov, T. Schmitt, U. Flechsig, T. Schmidt, A. Imhof, Q. Chen, J. Raabe, R. Betemps, D. Zimoch, J. Krempasky, X. Wang, M. Grioni, A. Piazzalunga, and L. Patthey, *Journal of Synchrotron Radiation* **17**, 631 (2010).
 - ³⁵ V. N. Strocov et. al, unpublished.
 - ³⁶ V. Hinkov, S. Pailhes, P. Bourges, Y. Sidis, A. Ivanov, A. Kulakov, D. P. Lin, C. T. Chen, C. Bernhard, and B. Keimer, *Nature (London)* **430**, 650 (2004).
 - ³⁷ K. Pasanai and W. A. Atkinson, *Phys. Rev. B* **81**, 134501 (2010).
 - ³⁸ D. H. Lu, D. L. Feng, N. P. Armitage, K. M. Shen, A. Damascelli, C. Kim, F. Ronning, Z.-X. Shen, D. A. Bonn, R. Liang, W. N. Hardy, A. I. Rykov, and S. Tajima, *Phys. Rev. Lett.* **86**, 4370 (2001).
 - ³⁹ A. Damascelli, D. H. Lu, K. M. Shen, N. P. Armitage, F. Ronning, D. L. Feng, C. Kim, Z.-X. Shen, T. Kimura, Y. Tokura, Z. Q. Mao, and Y. Maeno, *Phys. Rev. Lett.* **85**, 5194 (2000).
 - ⁴⁰ M. P. Seach and W. A. Dench, *Surface and interface analysis* **1**, 2 (1979).
 - ⁴¹ C. J. Powell, A. Jablonski, I. S. Tilinin, S. Tanuma, and D. R. Penn, *Journal of Electron Spectroscopy and Related Phenomena* **98-99**, 1 (1999).
 - ⁴² I. S. Tilinin, *Phys. Rev. B* **53**, 547 (1996).
 - ⁴³ E. D. Hansen, T. Miller, and T.-C. Chiang, *Phys. Rev. B* **55**, 1871 (1997).
 - ⁴⁴ E. E. Krasovskii, W. Schattke, P. Jiříček, M. Vondráček, O. V. Krasovska, V. N. Antonov, A. P. Shpak, and I. Bartoš, *Phys. Rev. B* **78**, 165406 (2008).
 - ⁴⁵ N. Barrett, E. E. Krasovskii, J.-M. Themlin, and V. N. Strocov, *Phys. Rev. B* **71**, 035427 (2005).
 - ⁴⁶ D. Fournier, G. Levy, Y. Pennec, J. L. McChesney, A. Bostwick, E. Rotenberg, R. Liang, W. N. Hardy, D. A. Bonn, I. S. Elfimov, and A. Damascelli, *Nature Phys.* **6**, 905 (2010).
 - ⁴⁷ Y. Sassa, M. Radović, M. Månsson, E. Razzoli, X. Y. Cui, S. Pailhès, S. Guerrero, M. Shi, P. R. Willmott, F. Miletto Granozio, J. Mesot, M. R. Norman, and L. Patthey, *Phys. Rev. B* **83**, 140511 (2011).
 - ⁴⁸ V. Zabolotnyy, S. Borisenko, A. Kordyuk, J. Geck, D. Inosov, A. Koitzsch, J. Fink, M. Knupfer, and B. B. *Physica C: Superconductivity* **460-462, Part 2**, 888 (2007).
 - ⁴⁹ D. Katagiri, K. Seki, R. Eder, and Y. Ohta, *Phys. Rev. B* **83**, 165124 (2011).
 - ⁵⁰ S. Basak, T. Das, H. Lin, J. Nieminen, M. Lindroos, R. S. Markiewicz, and A. Bansil, *Phys. Rev. B* **80**, 214520 (2009).
 - ⁵¹ D. S. Inosov, J. Fink, A. A. Kordyuk, S. V. Borisenko, V. B. Zabolotnyy, R. Schuster, M. Knupfer, B. Büchner, R. Follath, H. A. Dürr, W. Eberhardt, V. Hinkov, B. Keimer, and H. Berger, *Phys. Rev. Lett.* **99**, 237002 (2007).
 - ⁵² D. S. Inosov, R. Schuster, A. A. Kordyuk, J. Fink, S. V. Borisenko, V. B. Zabolotnyy, D. V. Evtushinsky, M. Knupfer, B. Büchner, R. Follath, and H. Berger, *Phys. Rev. B* **77**, 212504 (2008).
 - ⁵³ H. J. Levinson and E. W. Plummer, *Phys. Rev. B* **24**, 628 (1981).
 - ⁵⁴ B. C. Meyers and T. E. Feuchtwang, *Phys. Rev. B* **27**, 2030 (1983).
 - ⁵⁵ B. Feuerbacher and R. F. Willis, *Journal of Physics C: Solid State Physics* **9**, 169 (1976).
 - ⁵⁶ W. Sacks, D. Roditchev, and J. Klein, *Applied Physics A: Materials Science & Processing* **66**, S925 (1998).
 - ⁵⁷ P. A. Lee, T. M. Rice, and P. W. Anderson, *Solid State Communications* **14**, 703 (1974).